Accepted Manuscript

Design, synthesis and biochemical evaluation of novel multi-target inhibitors as potential anti-Parkinson agents

Simone Carradori, Francesco Ortuso, Anél Petzer, Donatella Bagetta, Celeste De Monte, Daniela Secci, Daniela De Vita, Paolo Guglielmi, Gokhan Zengin, Abdurrahman Aktumsek, Stefano Alcaro, Jacobus P. Petzer

PII: S0223-5234(17)30852-8

DOI: 10.1016/j.ejmech.2017.10.050

Reference: EJMECH 9842

To appear in: *European Journal of Medicinal Chemistry*

Received Date: 7 September 2017

Revised Date: 11 October 2017

Accepted Date: 16 October 2017

Please cite this article as: S. Carradori, F. Ortuso, Ané. Petzer, D. Bagetta, C. De Monte, D. Secci, D. De Vita, P. Guglielmi, G. Zengin, A. Aktumsek, S. Alcaro, J.P. Petzer, Design, synthesis and biochemical evaluation of novel multi-target inhibitors as potential anti-Parkinson agents, *European Journal of Medicinal Chemistry* (2017), doi: 10.1016/j.ejmech.2017.10.050.

This is a PDF file of an unedited manuscript that has been accepted for publication. As a service to our customers we are providing this early version of the manuscript. The manuscript will undergo copyediting, typesetting, and review of the resulting proof before it is published in its final form. Please note that during the production process errors may be discovered which could affect the content, and all legal disclaimers that apply to the journal pertain.

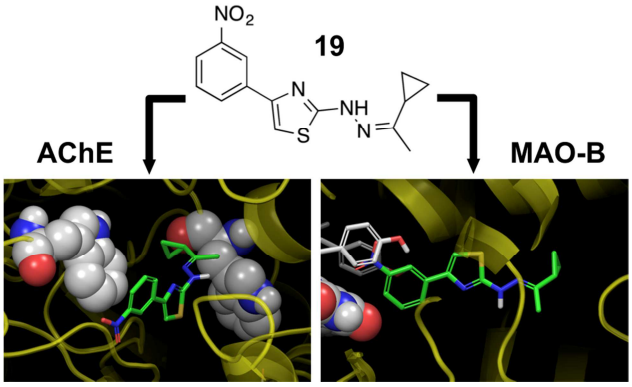

ACCEPTED MANUSCRIPT

ACCEPTED MANUSCRIPT

Design, synthesis and biochemical evaluation of novel multi-target inhibitors as potential anti-Parkinson agents

Simone Carradori [a], *Francesco Ortuso* [b,*], *Anél Petzer* [c], *Donatella Bagetta* [a], *Celeste De Monte* [d], *Daniela Secci* [d,*], *Daniela De Vita* [d], *Paolo Guglielmi* [d], *Gokhan Zengin* [e], *Abdurrahman Aktumsek* [e], *Stefano Alcaro* [b], *Jacobus P. Petzer* [c]

[a]Department of Pharmacy, "G. d'Annunzio" University of Chieti-Pescara, Via dei Vestini 31, 66100 Chieti, Italy

[b]Dipartimento di Scienze della Salute, University "Magna Graecia" of Catanzaro, Campus "S. Venuta", Viale Europa, 88100 Catanzaro, Italy

[c]Pharmaceutical Chemistry and Centre of Excellence for Pharmaceutical Sciences, North-West University, Potchefstroom 2520, South Africa

[d]Dipartimento di Chimica e Tecnologie del Farmaco, "Sapienza" University of Rome, P.le A. Moro 5, 00185 Rome, Italy

[e]Selcuk University, Science Faculty, Department of Biology, Konya, Turkey

*Corresponding authors

Email addresses: ortuso@unicz.it (F. Ortuso), daniela.secci@uniroma1.it (D. Secci)

ACCEPTED MANUSCRIPT

ABSTRACT

New 4-(3-nitrophenyl)thiazol-2-ylhydrazone derivatives are proposed as dual-target-directed monoamine oxidase B (MAO-B) and acetylcholinesterase (AChE) inhibitors, as well as antioxidant agents, for the treatment of neurodegenerative disorders such as Parkinson's disease. Rational molecular design, target recognition and predicted pharmacokinetic properties have been evaluated by means of molecular modelling. Based on these properties, compounds were synthesized and evaluated *in vitro* as MAO-B and AChE inhibitors, and compared to the activities at their corresponding isozymes, monoamine oxidase A (MAO-A) and butyrylcholinesterase (BuChE), respectively. Anti-oxidant properties, potentially useful in the treatment of neurodegenerative disorders, have been also investigated *in vitro*. Among the evaluated compounds, three inhibitors may be considered as promising dual inhibitors of MAO-B and AChE, *in vitro*. MAO-B inhibition was also shown to be competitive and reversible for compound **19**.

ACCEPTED MANUSCRIPT

1. Introduction

Parkinson's disease (PD) is a multifactorial, chronic neurodegenerative disorder with a high social impact, particularly in Western countries [1, 2]. The physiopathology of PD, even if not yet completely clear, reveals the deregulation of several genes, such as parkin, α-synuclein, DJ-1, leucine-rich repeat kinase 2, and PTEN-induced putative kinase 1, that may induce protein misfolding, phosphorylation and aggregation, mitochondrial dysfunction and oxidative stress [3]. In the early stages of PD these biochemical events result in the progressive loss of dopaminergic neurons in the central nervous system (CNS), particularly in the *pars compacta* of the *substantia nigra*. This pathology is associated with the appearance of intraneuronal protein aggregates known as Lewy bodies. In later phases of PD noradrenergic, serotonergic and cholinergic systems are also affected [3]. PD symptoms consisting in bradykinesia, resting tremor, muscle rigidity, and postural instability can be attributed to the loss of dopaminergic neurons while~~, in later phases,~~ cognitive decline, sleep abnormalities, and depression occur due to the involvement of the other neurotransmitter systems [4].

Currently, all available PD therapies are palliative and symptomatic, and their efficacy is strictly related to the stage of the pathology: early pharmacological treatments achieve the best results and may slow the disease development. Anti-Parkinson drugs, for the most part, act by increasing dopaminergic tone *via* the biosynthesis of the dopamine (i.e., L-DOPA), by stimulating dopamine receptors (i.e., Bromocriptine, Ropinirole), by limiting dopamine metabolism with the inhibition of COMT (i.e., Tolcapone) or MAO-B (i.e., Selegiline, Rasagiline, Safinamide) [5].

Moreover, considering that the MAO catalytic cycle produces several potentially neurotoxic species such as hydrogen peroxide, ammonia, and aldehydes, MAO-B inhibitors may reduce oxidative stress and neurotoxicity by reducing the formation of those metabolites [6]. While providing effective *in vivo* MAO inhibition, early MAO inhibitors (i.e., Phenelzine, Tranylcypromine and Isocarboxazide) possessed some safety problems. In contrast to more recent compounds, these drugs are not selective for a particular MAO isoform and their mechanism of inhibition is irreversible. Such nonselective irreversible MAO inhibitors prevent the peripheral metabolism of tyramine, which may lead to a potentially lethal hypertensive crisis known as "cheese effect" [7, 8]. Tyramine is an amine mostly present in cheese, red wine, meat

and fish, which dictates that dietary restrictions should be imposed when treatment with nonselective irreversible MAO inhibitors is initiated.

In the initial phase of PD, anti-muscarinic compounds can be administered to reduce extrapyramidal symptoms [3]. In drug resistant patients, surgical deep brain stimulation can be combined with pharmacological treatment [9]. To explain cognitive dysfunction in PD, a convergent *versus* parallel model, according to dopamine-acetylcholine dependent alterations in synaptic plasticity, has been proposed [10]. It has been suggested that AChE inhibitors, such as Rivastigmine and Donepezil, may be effective for the treatment of the psychotic and cognitive disorders associated with PD, without exacerbating motor symptoms [11, 12].

Due to its multifactorial physiopathology, the available PD treatments often require the co-administration of several drugs. With the aim to improve therapeutic efficacy and patient compliance, scientific research should be focused on a more promising multi-target-directed strategy with a single compound, appropriately designed, and addressing different pathological events [13, 14].

In the present study, taking into account our previous works [15-21], novel 4-(3-nitrophenyl)thiazol-2-ylhydrazones have been designed, synthesized and evaluated as dual-target-directed MAO-B and AChE inhibitors with reversible modes of inhibition according to the SAR studies proposed for this scaffold [22]. To investigate the abilities of the synthesized compounds to access the brain, their permeation across the blood-brain barrier (BBB) has been theoretically investigated and predicted *in silico*. Finally, the anti-oxidant properties of the compounds were investigated by five different assays *in vitro*. Based on the results of this study, three thiazolylhydrazones, **8**, **19** and **20**, were identified as promising lead compounds for the development of novel treatments for neurodegenerative disorders such as PD.

2. Results and discussion

2.1. Rational drug design

The molecular design workflow consisted of four steps: (a) first the shape and volume complementarity of the common scaffold were evaluated with respect to the targets, (b) then analyses of molecular interaction fields (MIFs) and quantum mechanics simulation suggested type and position of substituents, (c) pharmacokinetic properties of the designed compounds were theoretically predicted, and (d) finally the interaction of the MAOs and cholinesterases

(ChEs) with the proposed derivatives were investigated by means of docking experiments (Experimental section).

Because we have already demonstrated the MAO inhibitory properties of thiazolylhydrazone derivatives [23, 24], our goal was to rationally design new analogues that retain MAO-B inhibition, but also possessing inhibitory activity against ChEs. *Via* molecular modelling, the target recognition of the common scaffold, 4-(phenyl)thiazol-2-ylhydrazone (**1**) was firstly evaluated (Figure 1). In both MAO isoforms, **1** exhibited several binding modes, but in the most stable orientations the unsubstituted hydrazone moiety was directed towards the FAD cofactor, while the phenyl ring was located at the catalytic site entrance (Supplementary material, Figure S1a-b). The ChEs interacted with **1** principally by means of stacking contacts with Trp residues (Supplementary material, Figure S1c-d). In AChE, the external Trp286 was better recognized than the internal Trp86 residue, while in BuChE, where Ala277 replaces the AChE Trp286, **1** interacted with the internal Trp82 residue (corresponding to Trp86 in AChE). The binding orientation of **1** to the MAOs could allow for covalent bond formation between N5 of the FAD and the hydrazone group of **1**, which consequently could lead to irreversible target inhibition. In order to prevent such a possibility, two methyl groups were introduced to replace the hydrazone terminal hydrogen atoms, thus yielding compound **2** (Figure 1).

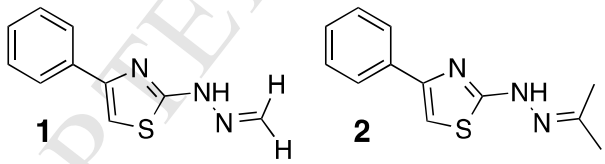

Fig. 1. Chemical structures of **1** and **2**.

The binding mode of **2** to MAO-A was completely opposite compared to **1**. In this instance, the phenyl ring was directed towards the FAD, thus excluding the possibility of covalent bond formation by means of the hydrazone moiety. Conversely, in MAO-B and the ChEs little difference was observed between the recognition of **1** and **2** (Supplementary material, Figure S2). In AChE, **2** slightly altered its position to interact with the inner Trp86 instead of the external Trp286, assuming a binding mode and position similar to that reported in the crystal structure 4EY7 for the interaction of AChE with the known selective inhibitor, Donepezil (Supplementary material, Figure S3) [25]. For the recognition of both **1** and **2**, the known key

role of stacking interactions was confirmed by graphical analysis. In order to improve such a favourable contribution, *ortho*-, *meta*- and *para*-nitrophenyl derivatives of **2** were designed according to the findings of molecular interaction fields (MIFs) analyses. Theoretical models, excluding ligands, for the MAOs and ChEs were mapped using ON GRID probe. The resulting MIFs were superimposed with the highest scored docking pose of **2** (Supplementary material, Figures S4 and S5). It was not surprising to observe a good correlation between the MAOs computed MIFs and all positions of the ligand phenyl moiety. In fact, the nitro group was already included at the *para* position, leading to improved interaction with the MAOs [21]. In contrast, the analyses of the MIFs of the ChEs suggested suitable substitution on the *ortho* and *meta* positions only. In view of the key role of stacking interactions in target recognition, we have investigated the effect of the position of nitro group on the coplanarity of the phenyl and thiazole rings. In fact, coplanar conformations allow for electron delocalization between the two aromatic rings, potentially improving stacking contacts to the targets. The relative energy profile as a function of the phenyl-thiazole dihedral angle (Figure 2) was computed using quantum mechanics methods (Experimental section).

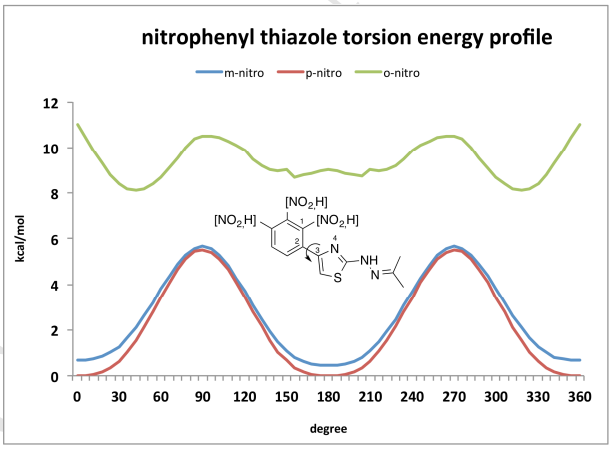

Fig. 2. The effect of the position of nitro group (*ortho*-, *meta*- and *para-)* on the relative energy profile of 4-(phenyl)thiazol-2-ylhydrazone scaffold as a function of the phenyl-thiazole dihedral angle.

The dihedral energy profiles clearly indicate that the nitro group at the *ortho* position prevents coplanarity of the phenyl and thiazolyl rings, while *meta*- and *para*-nitro derivatives allow for coplanarity, to the same degree. Considering the MIFs and quantum mechanics analysis, the

subsequent compounds were designed as *meta*-nitro derivatives only. In order to evaluate the effect of the nitro group on target recognition, compound **2** was substituted with the nitro group in the *meta* position to yield compound **3**. The new derivative was submitted to docking simulation as previously reported for **1** and **2**. The highest scored docking poses of **3** (Supplementary material, Figure S6) were similar to those of **2**, with some differences in theoretical target affinity (XP-GScore). The *m*-nitro derivative **3** exhibited similar interaction energies compared to precursor **2** at all targets except MAO-A. In this respect, the binding of compound **3** to MAO-A was weaker by 1.6 kcal/mol compared to **2**, thus providing better MAO-B selectivity, at least theoretically. In order to suggest novel and more potent dual-target-directed MAO-B and AChE inhibitors, known building blocks [20] were used to design a library of alkyl/cycloalkyl-substituted derivatives of **3** and the resulting structures were virtually screened against the MAO and ChE targets. The pharmacokinetics properties of the new compounds, such as oral absorption and blood-brain barrier permeation (Experimental section), and their interaction with the targets were computationally investigated (Table 1).

ACCEPTED MANUSCRIPT

Table 1. Chemical structures of the 4-(3-nitrophenyl)thiazol-2-ylhydrazones (**3**-**20**) and their theoretical properties and docking scores for binding to the MAOs and ChEs.

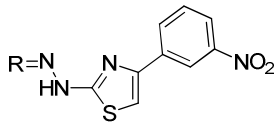

Compound	R	%OA[a]	QPlogBB[b]	*Docking score*[c]			
				MAO-A	MAO-B	AChE	BuChE
3		89.36	-0.92	-5.93	-7.15	-6.51	-7.31
4		92.59	-0.95	-5.92	-7.22	-6.59	-5.34
5		94.83	-1.05	-5.85	-8.06	-7.03	-6.79
6		96.41	-0.95	-2.59	-7.30	-6.58	-5.36
7		100.00	-1.00	0.56	-7.83	-7.68	-8.16
8	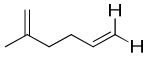	96.77	-1.14	0.50	-7.94	-7.65	-5.68
9	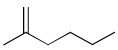	100.00	-1.15	-2.41	-8.14	-7.68	-5.73
10	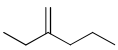	100.00	-1.05	0.28	-7.80	-7.39	-5.61
11	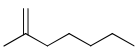	100.00	-1.25	-2.71	-8.87	-8.51	-8.37
12	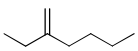	100.00	-1.15	0.01	-7.53	-9.28	-6.75
13	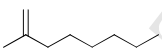	100.00	-1.35	-2.95	-9.05	-7.93	-8.60
14		92.84	-0.95	-6.71	-7.84	-6.45	-6.21
15		94.58	-0.92	-0.85	-7.60	-8.23	-7.13
16		100.00	-0.90	-1.26	-9.05	-9.88	-6.62
17		96.81	-0.90	0.61	-8.45	-8.98	-6.79
18		100.00	-0.83	1.79	-7.89	-8.29	-5.89
19		92.39	-0.97	-2.76	-7.98	-7.68	-6.68
20	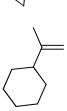	100.00	-0.97	0.76	-9.14	-7.26	-6.33

ACCEPTED MANUSCRIPT

[a]Percentage of oral dose absorbed; [b]Blood-brain barrier permeation as pLog(IN/OUT); [c]Best pose XP-GScore in kcal/mol.

The theoretical pharmacokinetic data correlated well with those of known CNS active drugs [26], and suggested that the 4-(3-nitrophenyl)thiazol-2-ylhydrazones could exhibit good absorption after oral administration, and could also penetrate the blood-brain. Analyses of the docking poses (Figures S7-S22) and scores suggested that these compounds could possess good MAO selectivity with a strong preference for the MAO-B isoform. This may be attributed to the productive hydrogen bond interaction between the thiazole ring nitrogen and the Cys172 in MAO-B, an interaction that is not possible in MAO-A since Asn181 is the corresponding residue in this position. Moreover, for compounds **7**, **8**, **10**, **12**, **17**, **18** and **20**, these results highlighted a disfavoured recognition of MAO-A as demonstrated by their target interaction energies greater than 0 kcal/mol. This finding suggests that the addition of steric hindrance at the hydrazone may be used to obtain MAO isoform selectivity. For the ChEs, the docking simulations did not suggest that the newly synthesized compounds will exhibit notable selectivity even if **4**, **8**-**10**, **12** and **16**-**20**, preferred AChE compared to BuChE. On the basis of the above theoretical analysis, derivatives **3**-**20** were selected for synthesis and *in vitro* biological evaluation.

2.2. Synthesis

4-(3-Nitrophenyl)thiazol-2-ylhydrazone derivatives (**3**-**20**) were synthesized in high yields as reported in our previous communications (Table 1) [27]. A carbonyl compound was reacted with thiosemicarbazide in ethanol at room temperature, with acetic acid serving as the catalyst (Scheme 1). Then, the resulting thiosemicarbazones were reacted in ethanol with 2-bromo-3'-nitroacetophenone to furnish the proposed derivatives by Hantzsch cyclization. All the synthesized products were washed with petroleum ether and diethyl ether and purified by column chromatography (ethyl acetate/petroleum ether) before characterization by spectroscopic methods (IR, ^{1}H and ^{13}C NMR) and elemental analysis to ensure high purity (≥96%).

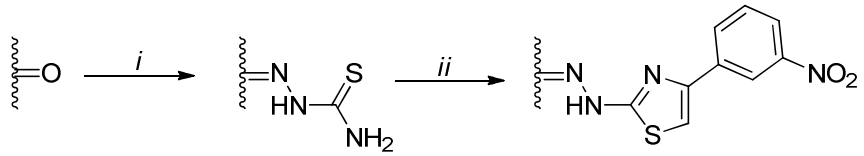

3-20

Scheme 1. Synthesis of 4-(3-nitrophenyl)thiazol-2-ylhydrazone derivatives **3-20**. Reagents and conditions: (i) thiosemicarbazide, EtOH, acetic acid (cat.), rt; (ii) 2-bromo-3'-nitroacetophenone, EtOH, rt.

2.3. In vitro MAO inhibition study

All the synthesized compounds were found to inhibit the human MAO enzymes, particularly the MAO-B isoform, with promising IC_{50} values. Several cycloaliphatic derivatives displayed inhibitory action against MAO-B at low nanomolar concentrations (Table 2). Conversely, these compounds inhibited MAO-A in the high micromolar range. Derivatives possessing linear aliphatic substituents (e.g. **1**, **2**, **8**-**11**) were particularly active MAO-B inhibitors (IC_{50} values ranging from 0.101 to 0.716 µM). Compounds substituted with a five-membered linear chain (**5**, **6**) or branched chain (**7**) exhibited very good MAO-B inhibition (IC_{50} values of 0.055, 0.053 and 0.012 µM, respectively). Among the cycloaliphatic substituents, the remarkable MAO-B inhibition was exhibited by cycloheptylidene **17** (IC_{50} = 0.0086 µM) and cyclooctylidene **18** (IC_{50} = 0.010 µM). The introduction of an exocyclic aliphatic ring improved the MAO-B inhibition potency and selectivity within this library with the cyclopropylethylidene **19** and cyclohexylethylidene **20** possessing IC_{50} values of 0.0053 µM and 0.0072 µM for MAO-B, respectively. These *in vitro* biological data thus supported the findings of the molecular modelling study, and showed that the 4-(3-nitrophenyl)thiazol-2-ylhydrazone derivatives were indeed potent MAO inhibitors with manifest selectivity for the MAO-B isoform.

Table 2. Inhibitory activities of compounds **3**-**20** towards MAO and ChE targets.

Compound	MAO-A[a]	MAO-B[a]	AChE[b]	BuChE[b]
3	1.07 ± 0.981	0.716 ± 0.521	3.00	12.85
4	20.5 ± 2.29	0.351 ± 0.043	14.00	12.13
5	38.0 ± 1.31	0.055 ± 0.0079	31.00	5.16
6	24.3 ± 2.91	0.053 ± 0.0074	9.00	7.45
7	4.41 ± 0.554	0.012 ± 0.0015	2.30	8.98
8	3.99 ± 0.218	0.101 ± 0.0089	47.00	6.35
9	6.33 ± 0.116	0.118 ± 0.021	24.00	11.34
10	4.86 ± 0.254	0.189 ± 0.017	15.00	11.02
11	7.15 ± 0.076	0.355 ± 0.035	5.28	8.68
12	6.03 ± 0.230	0.182 ± 0.030	10.00	10.01
13	10.9 ± 1.67	0.626 ± 0.053	3.00	9.54
14	3.46 ± 0.263	0.095 ± 0.014	14.15	12.44
15	2.56 ± 0.358	0.047 ± 0.0061	6.92	8.41
16	4.25 ± 0.237	0.237 ± 0.051	18.00	4.87
17	1.59 ± 0.201	0.0086 ± 0.0017	1.44	7.11
18	1.82 ± 0.061	0.010 ± 0.0061	0.80	7.64
19	2.66 ± 0.051	0.0053 ± 0.00080	44.00	12.77
20	29.1 ± 2.72	0.0072 ± 0.0018	41.00	6.22
Galantamine	-	-	13.44	13.62
Clorgyline	0.00446 ± 0.00032	61.35 ± 1.13	-	-
***R*-(-)-Deprenyl**	67.25 ± 1.02	0.01960 ± 0.00086	-	-

[a] IC_{50} values in μM; [b] percentage of target inhibition at 3 μM

The most potent MAO-B inhibitor of the series, compound **19**, was further investigated to determine if it acts as a reversible or irreversible MAO-B inhibitor. For this purpose, dialysis was used. MAO-B and compound **19** (at a concentration equal to 4 × IC_{50}) were combined and incubated for 15 min. The mixture was subsequently dialyzed for 24 h and diluted twofold, to yield a concentration of **19** equal to 2 × IC_{50}, and the residual enzyme activity was measured. As positive control, incubation and dialysis of MAO-B with the irreversible MAO-B inhibitor, (*R*)-(-)-deprenyl, were carried out while as negative control a similar experiment was carried out in absence of inhibitor. For comparison, the residual MAO activities of undialyzed mixtures of MAO-B and **19** were also measured after twofold dilution as above. The results of the dialysis study show that, after incubation with **19**, dialysis restores MAO-B activity to 91% of the

negative control value (Figure 3). This demonstrated that **19** is a reversible MAO-B inhibitor since, for reversible inhibition, dialysis is expected to restore enzyme activity to 100%. In contrast, after incubation with (*R*)-(-)-deprenyl, dialysis does not restore MAO-B activity with the residual activity at only 1.9%. In undialyzed mixtures, MAO-B inhibition persists with the activity at 46%.

Subsequently, Lineweaver-Burk plots for the inhibition of MAO-B by **19** were constructed to demonstrate that this compound is a competitive MAO-B inhibitor (Figure 3). Six Lineweaver-Burk plots were thus constructed at the following concentrations of **19**: 0 μM, ¼ × IC_{50}, ½ × IC_{50}, ¾ × IC_{50}, 1 × IC_{50} and 1¼ × IC_{50}. The Lineweaver-Burk plots were found to intersect on the y-axis, providing evidence of competitive inhibition and thus further supporting for a reversible interaction. From the replot of the slopes of the Lineweaver-Burk plots versus inhibitor concentration, a K_i value of 0.0073 μM for the inhibition of MAO-B by **19** was estimated.

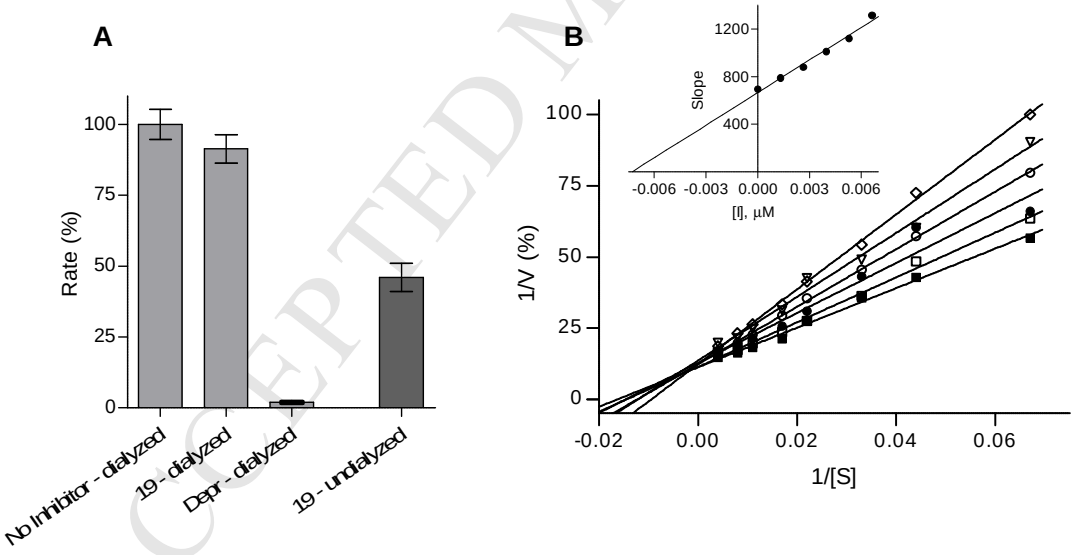

Fig. 3. A: Reversibility of the inhibition of MAO-B by **19**. MAO-B and **19** (at 4 × IC_{50}) were preincubated for 15 min, dialyzed for 24 h and the residual enzyme activity was measured (**19**-dialyzed). MAO-B was similarly preincubated in the absence (No inhibitor–dialyzed) and presence of the irreversible inhibitor, (*R*)-(-)-deprenyl (Depr-dialyzed), and dialyzed. For comparison, the residual MAO activity of undialyzed mixtures of MAO-B with **19** is also shown (**19**-undialyzed). B: Lineweaver-Burk plots of human MAO-B activities in the absence (filled

squares) and presence of various concentrations of compound **19**. The inset is a graph of the slopes of the Lineweaver-Burk plots versus inhibitor concentration.

2.4. In vitro cholinesterases inhibition study

To determine if the 4-(3-nitrophenyl)thiazol-2-ylhydrazones (**3**-**20**) may act as dual-target-directed inhibitors, they were also evaluated as potential AChE and BuChE inhibitors. For this purpose, Galantamine served as reference inhibitor, a compound which exhibits 13.44% and 13.62% inhibition of AChE and BuChE, respectively, at 3 µM. As reported in Table 2, all the compounds are moderate inhibitors of both ChE isoenzymes. Three derivatives, **8**, **19** and **20**, display the best inhibitory activity (>41%) of AChE at 3 µM, and also possess good selectivity for AChE over BuChE. These compounds may be considered as promising dual-target-directed inhibitors (MAO-B and AChE) for the treatment of neurodegenerative diseases as also previously reported [28].

2.5. Anti-oxidant in vitro assays

The *in vitro* anti-oxidant activity of this library (compounds **3**-**20**) has been evaluated by five experimental approaches, using trolox as a reference compound. Among free radical scavenging methods, DPPH assay is highly sensitive, simple and not costly. In addition, ABTS test could be applicable to both hydrophilic and lipophilic compounds. The free radical scavenging potential of the 4-(3-nitrophenyl)thiazol-2-ylhydrazones was slightly lower than trolox, whereas in the reducing power (important for the inhibition of the Fenton reaction between metal ions and the byproducts of MAO-mediated reaction) and total anti-oxidant capacity in the phosphomolybdenum (PhosphoMo) assay, the test and reference compounds display almost comparable potencies. These ancillary biological activities could be useful for the treatment of multifactorial neurodegenerative diseases where oxidative stress enhances cognitive impairment and inflammatory processes.

Table 3. Anti-oxidant activities of compounds **3-20** compared to the reference drug trolox.

Compound	Anti-oxidant assays				
	PhosphoMo[a]	FRAP[a]	CUPRAC[a]	DPPH[b]	ABTS[b]
3	1.75 ± 0.08	0.34 ± 0.01	0.51 ± 0.02	1.16 ± 0.03	1.07 ± 0.02
4	1.65 ± 0.13	0.42 ± 0.01	0.58 ± 0.01	1.18 ± 0.02	1.04 ± 0.01
5	1.20 ± 0.08	0.45 ± 0.01	0.55 ± 0.05	1.20 ± 0.02	1.04 ± 0.01
6	1.10 ± 0.02	0.34 ± 0.01	0.46 ± 0.02	1.13 ± 0.01	1.04 ± 0.01
7	1.13 ± 0.03	0.42 ± 0.01	0.57 ± 0.01	1.35 ± 0.01	1.05 ± 0.02
8	1.15 ± 0.05	0.33 ± 0.01	0.46 ± 0.02	1.21 ± 0.01	1.04 ± 0.01
9	1.46 ± 0.06	0.37 ± 0.01	0.52 ± 0.02	1.18 ± 0.02	1.06 ± 0.02
10	1.25 ± 0.02	0.39 ± 0.02	0.53 ± 0.02	1.23 ± 0.02	1.04 ± 0.01
11	1.47 ± 0.08	0.37 ± 0.05	0.59 ± 0.09	1.17 ± 0.09	1.05 ± 0.07
12	1.56 ± 0.04	0.41 ± 0.02	0.55 ± 0.01	1.26 ± 0.02	1.04 ± 0.01
13	1.24 ± 0.08	0.39 ± 0.01	0.53 ± 0.01	1.15 ± 0.01	1.11 ± 0.10
14	1.34 ± 0.01	0.40 ± 0.03	0.51 ± 0.03	1.18 ± 0.04	1.10 ± 0.09
15	1.43 ± 0.07	0.33 ± 0.01	0.32 ± 0.01	1.20 ± 0.02	1.10 ± 0.08
16	1.13 ± 0.08	0.39 ± 0.01	0.39 ± 0.02	1.18 ± 0.01	1.09 ± 0.07
17	1.23 ± 0.03	0.42 ± 0.03	0.41 ± 0.02	1.22 ± 0.01	1.07 ± 0.05
18	1.22 ± 0.09	0.39 ± 0.02	0.44 ± 0.03	1.28 ± 0.02	1.09 ± 0.08
19	1.47 ± 0.07	0.47 ± 0.02	0.53 ± 0.02	1.26 ± 0.02	1.06 ± 0.03
20	1.19 ± 0.03	0.67 ± 0.03	0.61 ± 0.01	1.35 ± 0.01	1.05 ± 0.02
Trolox	1.13 ± 0.05	0.16 ± 0.01	0.24 ± 0.02	0.40 ± 0.01	0.66 ± 0.02

[a]EC_{50} values in mM; [b]IC_{50} values in mM.

2.6. Pan Assay INterference compoundS (PAINS) evaluation

Compounds **3-20**, due to their chemical scaffold, dual inhibition and modest anti-oxidant properties could be suspected of artificial activity. In view of this, and according to a recently published editorial [29], all designed inhibitors have been evaluated by means of three different theoretical tools such as ZINC PAINS Pattern Identifier [30], False Positive Remover [31] and FAF-Drug4 [32]. None of the considered algorithms reported our compounds as potential PAINS or covalent inhibitors. ZINC PAINS Pattern Identifier suggested **3**, **4** and **6** to be further investigated by means of aggregation tests only. Because **3**, **4** and **6** have not demonstrated interesting activities *in vitro*, the evaluation of their aggregative properties has been not carried out. A further indication that our compounds are not PAINS can be taken from their experimental activities: **3-20**, in general, discriminated between target isoforms. Finally, the

inhibition of MAO-B, affected by compound **19**, has been demonstrated as a competitive and reversible process. Taking into account the above reported results and considerations, we are confident that our designed inhibitors, in particular the most promising **8**, **19** and **20**, did not show artificial activities.

3. Conclusions

A multidisciplinary approach allowed the identification of three new promising dual inhibitors that could be useful in Parkinson's disease therapy. A molecular modelling-based rational drug design approach has driven the synthesis of a small library of 4-(3-nitrophenyl)thiazol-2-ylhydrazone derivatives. Experimental evaluations have confirmed, *in vitro*, the inhibition of both MAO-B and AChE, and the selectivity with respect to the corresponding MAO-A and BuChE isozymes. Anti-oxidant properties of these new inhibitors have been also demonstrated, thus highlighting a useful synergistic effect for the treatment of neurodegenerative disorders. Further study, based on these results, will be carried out to investigate the biological properties of the identified inhibitors on cell lines and *in vivo* models.

4. Experimental protocols

4.1. Molecular modelling

Theoretical studies were performed using the Schrödinger Suite version 2015-4 [33]. The three-dimensional models of the designed compounds were built using the Maestro GUI [34] and optimized by means of the OPLS-2005 force field [35] Solvent effects were taken into account using the GB/SA water implicit solvation model [36] Target theoretical structures were obtained from Protein Data Bank (PDB) [37]: crystallographic entries 2Z5X [38], 2V5Z [39], 4M0E [40], and 1P0I [41] for MAO-A, MAO-B, AChE and BuChE, respectively. In order to prepare the models for simulation, all PDB entries were submitted to a preliminary pre-treatment: ligands and co-crystallized water molecules were removed, missing hydrogen atoms were added and, in the MAO targets, FAD connectivity was fixed. Torsion energy profiles of *ortho*-, *meta*- or *para*-substituted nitrophenyl ring with respect to the thiazole ring were investigated at DTF level of theory using the B3LYP functional and the 6-31G** basis set, as implemented in Jaguar software [42]. For each isomer, the torsion scan was carried out from 0° to 360° degree at regular intervals of 6°. The energy of the corresponding 61 conformers, for each derivative, was computed after

optimisation *in vacuo*. Molecular interaction fields (MIFs) analysis was performed by applying the program GRID [43, 44] to the structure models of the MAOs and ChEs. ON and C3 probes were used to highlight target favourable interaction areas for nitro and methyl substituents, respectively. The resolution of the computed MIFs was fixed at 0.33 Å (NPLA=3). Other GRID directives were left to default values. Oral bioavailability (as %) and BBB permeation [26] were computed using the QikProp tool [45]. Docking experiments were carried out with the Glide software [46]. Target binding sites were defined by means of a regular grid box of about 64,000 $Å^3$ centred in the MAOs, on the FAD N5 atom and in the ChEs, on the catalytic serine residue. All simulations were computed using Glide ligand flexible algorithm at extra-precision (XP) level. Authors will release the atomic coordinates and experimental data upon article publication.

4.2. Chemistry

Starting materials and reagents used in the synthetic procedures were obtained from commercial suppliers and were used without purification. Where mixtures of solvents are specified, the stated ratios are volume:volume. All melting points were measured on a Stuart® melting point apparatus SMP1, and are uncorrected. Temperatures are reported in °C. ^1H and ^{13}C NMR spectra were recorded at 400 MHz and 101 MHz, respectively, on a Bruker spectrometer using $CDCl_3$ and DMSO-d_6 as the solvents. Chemical shifts are expressed as δ units (parts per million) relative to the solvent signal. Coupling constants J are given in Hertz (Hz). IR (neat) spectra were recorded on a FT-IR Perkin-Elmer SpectrumOne instrument with the ATR system. Absorption bands (ν_{max}) are reported as the wavenumbers (cm^{-1}). Elemental analyses for C, H, and N were recorded on a Perkin-Elmer 240 B microanalyzer and the analytical results were within ± 0.4% of the theoretical values for all compounds. All reactions were monitored by TLC performed on 0.2 mm thick silica gel plates (60 F_{254}, Merck). Visualization was carried out under UV irradiation (254 nm). Preparative flash column chromatography was carried out on silica gel (high purity grade, pore size 60 Å, 200-425 mesh particle size). Organic solutions were dried over anhydrous sodium sulfate. Evaporation of the solvent after reaction was carried out on a rotary evaporator (Büchi Rotavapor). Where given, systematic compound names are those generated by ChemBioDraw Ultra® 12.0 following IUPAC conventions.

4.3. General synthetic procedure

The appropriate carbonyl compound (1.0 equiv.) was dissolved in 50 mL of ethanol and magnetically stirred with an equimolar amount of thiosemicarbazide for 24-72 h at room

temperature, using acetic acid as the catalyst. The obtained suspension was filtered, and the solid washed consecutively with petroleum ether and diethyl ether. The thiosemicarbazone (1.0 equiv.) thus obtained was reacted with 2-bromo-3'-nitroacetophenone dissolved in ethanol (50 mL) under magnetic stirring at room temperature for 24-72 h. The reaction was monitored by TLC until completion. The resulting 4-(3-nitrophenyl)thiazol-2-ylhydrazone derivative was collected by filtration, washed with petroleum ether and diethyl ether, and purified by column chromatography using ethyl acetate:petroleum ether as mobile phase, to give compounds **3**-**20** in good yields. Chemical-physical data are characteristic for the most predominant *E* geometric isomer because of the upshielding observed in the ^{1}H NMR spectra for the NH signal and for the absence of any *Z*-stabilizing functional groups [27].

In general, the IR spectrum (neat) for derivatives **3**-**20** showed stretching absorption bands at approximately 3300 cm^{-1} for NH, at 3030 cm^{-1} due to the stretching of C_{sp2}-H, at 1630 cm^{-1} for the C=N and at 1580 and 1440 cm^{-1} for C=C.

*4.4. Characterization data for compounds **3**-**20***

*4.4.1. 1-(4-(3-Nitrophenyl)thiazol-2-yl)-2-(propan-2-ylidene)hydrazine (**3**)* [47]

*4.4.2. 1-(Butan-2-ylidene)-2-(4-(3-nitrophenyl)thiazol-2-yl)hydrazine (**4**)*

Yellow powder, mp 165-170 °C, 73% yield; ^{1}H NMR (400 MHz, $CDCl_3$): δ 1.16-1.19 (t, 3H, CH_3), 2.20 (s, 3H, CH_3), 2.43-2.45 (q, 2H, CH_2), 6.95 (s, 1H, C_5H-thiazole), 7.74-7.77 (m, 1H, Ar), 8.18-8.20 (m, 1H, Ar), 8.24-8.27 (m, 1H, Ar), 8.52 (s, 1H, Ar), 12.31 (bs, 1H, NH, D_2O exch.). ^{13}C NMR (101 MHz, DMSO-d_6): δ 11.0 (CH_3), 16.9 (CH_3), 31.6 (CH_2), 106.6 (Ar-C_5, thiazole), 120.4 (Ar), 122.4 (Ar), 130.6 (Ar), 132.0 (Ar), 136.6 (Ar), 147.9 (Ar-NO_2), 148.7 (Ar-C_4, thiazole), 154.7 (C=N), 170.9 (C=N, thiazole).

*4.4.3. 1-(4-(3-Nitrophenyl)thiazol-2-yl)-2-(pentan-2-ylidene)hydrazine (**5**)*

Green powder, mp 175-179 °C, 64% yield; ^{1}H NMR (400 MHz, $CDCl_3$): δ 0.97-1.00 (m, 3H, CH_3), 1.64-1.68 (m, 2H, CH_2), 2.18 (s, 3H, CH_3), 2.36-2.40 (m, 2H, CH_2), 6.94 (s, 1H, C_5H-thiazole), 7.54-7.56 (m, 1H, Ar), 8.29-8.32 (m, 2H, Ar), 8.53 (s, 1H, Ar), 12.23 (s, 1H, NH, D_2O exch.). ^{13}C NMR (101 MHz, DMSO-d_6): δ 14.0 (CH_3), 16.9 (CH_3), 19.6 (CH_2), 32.8 (CH_2), 106.0 (Ar-C_5, thiazole), 120.4 (Ar), 122.4 (Ar), 130.3 (Ar), 132.0 (Ar), 136.6 (Ar), 147.9 (Ar-NO_2), 148.8 (Ar-C_4, thiazole), 153.6 (C=N), 166.0 (C=N, thiazole).

*4.4.4. 1-(4-(3-Nitrophenyl)thiazol-2-yl)-2-(pentan-3-ylidene)hydrazine (**6**)*

Green powder, mp 177-179 °C, 76% yield; ^{1}H NMR (400 MHz, $CDCl_3$): δ 1.15-1.28 (t, 6H, 2 x CH_3), 2.43-2.45 (q, 2H, CH_2), 2.54-2.56 (q, 2H, CH_2), 6.95 (s, 1H, C_5H-thiazole), 7.74-7.76 (m, 1H, Ar), 8.26-8.30 (m, 1H, Ar), 8.35-8.37 (m, 1H, Ar) , 8.52 (s, 1H, Ar), 12.32 (s, 1H, NH, D_2O exch.). ^{13}C NMR (101 MHz, DMSO-d_6): δ 10.2 (CH_3), 11.0 (CH_3), 23.2 (CH_2), 29.0 (CH_2), 106.6 (Ar-C_5, thiazole), 120.4 (Ar), 122.3 (Ar), 130.6 (Ar), 132.0 (Ar), 136.6 (Ar), 148.2 (Ar-NO_2), 148.7 (Ar-C_4, thiazole), 155.6 (C=N), 171.1 (C=N, thiazole).

*4.4.5. 1-(4-Methylpentan-2-ylidene)-2-(4-(3-nitrophenyl)thiazol-2-yl)hydrazine (**7**)*

Brown oil, 64% yield; ^{1}H NMR (400 MHz, $CDCl_3$): δ 0.97-0.99 (d, J = 6.8 Hz, 6H, 2 x CH_3), 1.90 (s, 3H, CH_3), 2.01-2.02 (m, 1H, CH), 2.21-2.23 (d, J = 7.2 Hz, 2H, CH_2), 7.02 (s, 1H, C_5H-thiazole), 7.53-7.57 (t, 1H, Ar), 8.11-8.15 (t, 2H, Ar), 8.40 (bs, 1H, NH, D_2O exch.), 8.66 (s, 1H, Ar). ^{13}C NMR (101 MHz, DMSO-d_6): δ 17.1 (CH_3), 22.8 (2 x CH_3), 25.8 (CH), 47.5 (CH_2), 106.6 (Ar-C_5, thiazole), 120.4 (Ar), 122.4 (Ar), 130.6 (Ar), 132.0 (Ar), 136.8 (Ar), 148.3 (Ar-NO_2), 148.7 (Ar-C_4, thiazole), 153.0 (C=N), 170.9 (C=N, thiazole).

*4.4.6. 1-(Hex-5-en-2-ylidene)-2-(4-(3-nitrophenyl)thiazol-2-yl)hydrazine (**8**)*

Yellow powder, mp 180-182 °C, 71% yield; ^{1}H NMR (400 MHz, $CDCl_3$): δ 2.19 (s, 3H, CH_3), 2.37-2.39 (m, 2H, CH_2), 2.49-2.51 (m, 2H, CH_2), 5.04-5.06 (m, 2H, =CH_2), 5.90-5.94 (m, 1H, =CH), 6.96 (s, 1H, C_5H-thiazole), 7.54-7.56 (m, 1H, Ar), 8.19-8.21 (d, J = 7.4 Hz, 1H, Ar), 8.30-8.31 (d, J = 7.4 Hz, 1H, Ar), 8.52 (s, 1H, Ar), 12.27 (bs, 1H, NH, D_2O exch.). ^{13}C NMR (101 MHz, DMSO-d_6): δ 17.1 (CH_3), 30.3 (CH_2), 37.6 (CH_2), 106.6 (Ar-C_5, thiazole), 115.6 (=CH_2), 120.4 (Ar), 122.4 (Ar), 130.6 (Ar), 132.0 (Ar), 136.6 (Ar), 138.3 (=CH-), 148.0 (Ar-NO_2), 149.0 (Ar-C_4, thiazole), 152.9 (C=N), 170.8 (C=N, thiazole).

*4.4.7. 1-(Hexan-2-ylidene)-2-(4-(3-nitrophenyl)thiazol-2-yl)hydrazine (**9**)*

Green powder, mp 156-160 °C, 82% yield; ^{1}H NMR (400 MHz, DMSO-d_6): δ 0.89-0.93 (m, 3H, CH_3), 1.32-1.35 (m, 2H, CH_2), 1.49-1.53 (m, 2H, CH_2), 1.93 (s, 3H, CH_3), 2.23-2.27 (m, 2H, CH_2), 7.56 (s, 1H, C_5H-thiazole), 7.68-7.73 (m, 1H, Ar), 8.13-8.15 (m, 1H, Ar), 8.28-8.31 (m, 1H, Ar), 8.70 (s, 1H, Ar), 10.80 (bs, 1H, NH, D_2O exch.). ^{13}C NMR (101 MHz, DMSO-d_6): δ 14.3 (CH_3), 17.0 (CH_3), 22.2 (CH_2), 28.3 (CH_2), 38.0 (CH_2), 106.6 (Ar-C_5, thiazole), 120.4 (Ar), 122.6 (Ar), 130.6 (Ar), 132.0 (Ar), 137.0 (Ar), 148.2 (Ar-NO_2), 148.7 (Ar-C_4, thiazole), 156.6 (C=N), 170.9 (C=N, thiazole).

*4.4.8. 1-(Hexan-3-ylidene)-2-(4-(3-nitrophenyl)thiazol-2-yl)hydrazine (**10**)*

Yellow powder, mp 153-155 °C, 84% yield; ^{1}H NMR (400 MHz, DMSO-d_6): δ 0.92-0.96 (m, 3H, CH_3), 1.03-1.08 (m, 3H, CH_3), 1.48-1.50 (m, 2H, CH_2), 2.23-2.30 (m, 2H, CH_2), 2.33-2.37 (m, 2H, CH_2), 7.56 (s, 1H, C_5H-thiazole), 7.68-7.77 (m, 1H, Ar), 8.13-8.15 (m, 1H, Ar), 8.28-8.30 (m, 1H, Ar), 8.70 (s, 1H, Ar), 11.00 (bs, 1H, NH, D_2O exch.). ^{13}C NMR (101 MHz, DMSO-d_6): δ 11.0 (CH_3), 14.4 (CH_3), 19.5 (CH_2), 29.5 (CH_2), 37.8 (CH_2), 106.6 (Ar-C_5, thiazole), 120.4 (Ar), 122.4 (Ar), 130.6 (Ar), 132.0 (Ar), 136.6 (Ar), 148.0 (Ar-NO_2), 148.7 (Ar-C_4, thiazole), 157.3 (C=N), 171.0 (C=N, thiazole).

*4.4.9. 1-(Heptan-2-ylidene)-2-(4-(3-nitrophenyl)thiazol-2-yl)hydrazine (**11**)*

Green powder, mp 79-81 °C, 73% yield; ^{1}H NMR (400 MHz, slightly soluble in DMSO-d_6): δ 0.85-0.89 (m, 3H, CH_3), 1.25-1.30 (m, 4H, 2 x CH_2), 1.49-1.51 (m, 2H, CH_2), 1.91 (s, 3H, CH_3), 2.20-2.24 (t, 2H, CH_2), 7.55 (s, 1H, C_5H-thiazole), 7.69-7.71 (m, 1H, Ar), 8.11-8.14 (m, 1H, Ar), 8.27-8.29 (m, 1H, Ar), 8.67 (s, 1H, Ar), 10.83 (bs, 1H, NH, D_2O exch.).

*4.4.10. 1-(Heptan-3-ylidene)-2-(4-(3-nitrophenyl)thiazol-2-yl)hydrazine (**12**)*

Brown oil, 69% yield; ^{1}H NMR (400 MHz, $CDCl_3$): δ 0.97-1.00 (m, 3H, CH_3), 1.17-1.20 (t, 3H, CH_3), 1.39-1.47 (m, 2H, CH_2), 1.53-1.68 (m, 2H, CH_2), 2.25-2.40 (m, 4H, CH_2), 7.02 (s, 1H, C_5H-thiazole), 7.54-7.58 (t, 1H, Ar), 8.11-8.15 (m, 2H, Ar), 8.44 (bs, 1H, NH, D_2O exch.), 8.67 (s, 1H, Ar). ^{13}C NMR (101 MHz, DMSO-d_6): δ 10.2 (CH_3), 14.3 (CH_3), 22.7 (CH_2), 25.8 (CH_2), 27.6 (CH_2), 35.4 (CH_2), 106.6 (Ar-C_5, thiazole), 120.4 (Ar), 122.7 (Ar), 130.6 (Ar), 132.0 (Ar), 136.6 (Ar), 147.8 (Ar-NO_2), 148.6 (Ar-C_4, thiazole), 158.2 (C=N), 171.0 (C=N, thiazole).

*4.4.11. 1-(Octan-2-ylidene)-2-(4-(3-nitrophenyl)thiazol-2-yl)hydrazine (**13**)*

Yellow powder, mp 135-137 °C, 81% yield; ^{1}H NMR (400 MHz, DMSO-d_6): δ 0.85-0.88 (m, 3H, CH_3), 1.28-1.29 (m, 6H, 3 x CH_2), 1.49-1.53 (m, 2H, CH_2), 1.92 (s, 3H, CH_3), 2.22-2.25 (m, 2H, CH_2), 7.57 (s, 1H, C_5H-thiazole), 7.68-7.74 (m, 1H, Ar), 8.12-8.15 (m, 1H, Ar), 8.28-8.30 (m, 1H, Ar), 8.68-8.69 (m, 1H, Ar), 10.84 (bs, 1H, NH, D_2O exch). ^{13}C NMR (101 MHz, DMSO-d_6): δ 14.4 (CH_3), 17.0 (CH_3), 22.5 (CH_2), 26.1 (CH_2), 28.7 (CH_2), 31.6 (CH_2), 38.3 (CH_2), 106.6 (Ar-C_5, thiazole), 120.4 (Ar), 122.4 (Ar), 130.6 (Ar), 132.0 (Ar), 136.6 (Ar), 145.3 (Ar-NO_2), 148.7 (Ar-C_4, thiazole), 153.8 (C=N), 170.9 (C=N, thiazole).

*4.4.12. 1-Cyclopentylidene-2-(4-(3-nitrophenyl)thiazol-2-yl)hydrazine (**14**)* [47]

*4.4.13. 1-Cyclohexylidene-2-(4-(3-nitrophenyl)thiazol-2-yl)hydrazine (**15**)*

Grey powder, mp 178-185 °C, 69% yield; ^{1}H NMR (400 MHz, $CDCl_3$): δ 1.68-1.70 (m, 2H, cyclohexane), 1.78-1.81 (m, 4H, cyclohexane), 2.41-2.44 (m, 2H, cyclohexane), 2.61-2.64 (m,

2H, cyclohexane), 6.94 (s, 1H, C_5H-thiazole), 7.74-7.75 (m, 1H, Ar), 8.20-8.25 (m, 2H, Ar), 8.52 (s, 1H, Ar), 12.28 (bs, 1H, NH, D_2O exch.). ^{13}C NMR (101 MHz, DMSO-d_6): δ 25.5 (CH_2), 26.0 (CH_2), 27.3 (CH_2), 27.7 (CH_2), 35.2 (CH_2), 106.5 (Ar-C_5, thiazole), 120.5 (Ar), 122.4 (Ar), 130.6 (Ar), 132.1 (Ar), 136.4 (Ar), 147.7 (Ar-NO_2), 148.7 (Ar-C_4, thiazole), 156.8 (C=N), 170.8 (C=N, thiazole).

*4.4.14. 2-(2-(4-methylcyclohexylidene)hydrazinyl)-4-(3-nitrophenyl)thiazole (**16**)*

Grey powder, mp 174-176 °C, 78% yield; ^{1}H NMR (400 MHz, $CDCl_3$): δ 0.98-0.99 (d, 3H, J = 6.5 Hz, CH_3), 1.24-1.25 (m, 2H, cyclohexane), 1.34-1.45 (m, 2H, cyclohexane), 1.57-1.66 (m, 2H, cyclohexane), 1.90-2.01 (m, 1H, cyclohexane), 2.20-3.20 (m, 2H, cyclohexane), 6.67 (s, 1H, C_5H-thiazole), 7.01 (s, 1H, Ar), 7.26-7.29 (m, 2H, Ar), 7.30-7.41 (m, 1H, Ar), 12.24 (bs, 1H, NH, D_2O exch.). ^{13}C NMR (400 MHz, DMSO-d_6): ^{13}C NMR (101 MHz, DMSO-d_6): δ 21.8 (CH_3), 26.9 (CH_2), 31.5 (CH), 34.0 (CH_2), 34.4 (CH_2), 35.3 (CH_2), 106.5 (Ar-C_5, thiazole), 120.4 (Ar), 122.4 (Ar), 130.6 (Ar), 132.1 (Ar), 136.6 (Ar), 147.8 (Ar-NO_2), 148.7 (Ar-C_4, thiazole), 156.5 (C=N), 170.8 (C=N, thiazole).

*4.4.15. 1-Cycloheptylidene-2-(4-(3-nitrophenyl)thiazol-2-yl)hydrazine (**17**)*

White powder, mp 194-195 °C, 83% yield; ^{1}H NMR (400 MHz, $CDCl_3$): δ 1.64-1.71 (m, 6H, cycloheptane), 1.86-1.87 (m, 2H, cycloheptane), 2.57-2.59 (m, 2H, cycloheptane), 2.69-2.71 (m, 2H, cycloheptane), 6.96 (s, 1H, C_5H-thiazole), 7.75-7.77 (m, 1H, Ar), 8.19-8.31 (m, 2H, Ar), 8.52 (s, 1H, Ar), 12.11 (bs, 1H, NH, D_2O exch.). ^{13}C NMR (101 MHz, DMSO-d_6): δ 24.5 (CH_2), 27.7 (CH_2), 30.3 (CH_2), 30.3 (CH_2), 31.4 (CH_2), 36.8 (CH_2), 106.7 (Ar-C_5, thiazole), 120.5 (Ar), 122.4 (Ar), 130.6 (Ar), 132.1 (Ar), 136.5 (Ar), 147.7 (Ar-NO_2), 148.7 (Ar-C_4, thiazole), 159.4 (C=N), 170.7 (C=N, thiazole).

*4.4.16. 1-Cyclooctylidene-2-(4-(3-nitrophenyl)thiazol-2-yl)hydrazine (**18**)*

Yellow powder, mp 180-183 °C, 81% yield; ^{1}H NMR (400 MHz, $CDCl_3$): δ 1.43-1.44 (m, 2H, cyclooctane), 1.57-1.59 (m, 4H, cyclooctane), 1.85-1.86 (m, 2H, cyclooctane), 1.96-1.98 (m, 2H, cyclooctane), 2.48-2.51 (m, 2H, cyclooctane), 2.62-2.65 (m, 2H, cyclooctane), 6.94 (s, 1H, C_5H-thiazole), 7.76-7.78 (m, 1H, Ar), 8.21-8.22 (m, 1H, Ar), 8.29-8.32 (m, 1H, Ar), 8.52 (s, 1H, Ar), 12.33 (bs, 1H, NH, D_2O exch.). ^{13}C NMR (101 MHz, DMSO-d_6): δ 24.1 (CH_2), 25.3 (CH_2), 25.5 (CH_2), 26.7 (CH_2), 27.3 (CH_2), 28.5 (CH_2), 36.1 (CH_2), 106.6 (Ar-C_5, thiazole), 120.5 (Ar), 122.5 (Ar), 130.6 (Ar), 132.1 (Ar), 136.4 (Ar), 147.6 (Ar-NO_2), 148.7 (Ar-C_4, thiazole), 160.1 (C=N), 170.6 (C=N, thiazole).

*4.4.17. 1-(1-Cyclopropylethylidene)-2-(4-(3-nitrophenyl)thiazol-2-yl)hydrazine (**19**)*

Yellow powder, mp 150-155 °C, 89% yield; ^{1}H NMR (400 MHz, DMSO-d_6): δ 0.72-0.75 (m, 4H, cyclopropane), 1.64-1.67 (m, 1H, cyclopropane), 1.79 (bs, 3H, CH_3), 7.55 (s, 1H, C_5H-thiazole), 7.69 (t, *J*= 8.0 Hz, 1H, Ar), 8.13 (d, *J*= 8.0 Hz, 1H, Ar), 8.27 (d, *J*= 7.6 Hz, 1H, Ar), 8.66 (s, 1H, Ar), 10.90 (bs, 1H, NH, D_2O exch.). ^{13}C NMR (101 MHz, DMSO-d_6): δ 6.2 (2 x CH_2, cyclopropane), 14.7 (CH, cyclopropane), 18.0 (CH_2), 106.5 (Ar-C_5, thiazole), 120.4 (Ar), 122.4 (Ar), 130.6 (Ar), 132.0 (Ar), 136.5 (Ar), 147.8 (Ar-NO_2), 148.7 (Ar-C_4, thiazole), 155.4 (C=N), 170.7 (C=N, thiazole).

*4.4.18. 1-(1-Cyclohexylethylidene)-2-(4-(3-nitrophenyl)thiazol-2-yl)hydrazine (**20**)*

White powder, mp 177-179 °C, 78% yield; ^{1}H NMR (400 MHz, $CDCl_3$): δ 1.31-1.36 (m, 5H, cyclohexane), 1.84-1.87 (m, 5H, cyclohexane), 2.13 (s, 3H, CH_3), 2.16-2.19 (m, 1H, cyclohexane), 6.95 (s, 1H, C_5H-thiazole), 7.71-7.74 (t, 1H, Ar), 8.17-8.19 (d, *J*= 8.0 Hz, 1H, Ar), 8.27-8.29 (d, *J* = 8.0 Hz, 1H, Ar), 8.53 (s, 1H, Ar), 11.91 (bs, 1H, NH, D_2O exch.). ^{13}C NMR (101 MHz, DMSO-d_6): δ 15.5 (CH_2), 26.0 (2 x CH_2, cyclohexane), 30.3 (2 x CH_2, cyclohexane), 46.3 (CH_3), 106.7 (Ar-C_5, thiazole), 120.4 (Ar), 122.3 (Ar), 130.6 (Ar), 132.0 (Ar), 136.8 (Ar), 148.2 (Ar-NO_2), 148.7 (Ar-C_4, thiazole), 156.6 (C=N), 171.1 (C=N, thiazole).

4.5. MAO-A and MAO-B inhibition studies

IC_{50} values for the inhibition of MAO-A and MAO-B were measured according to the literature protocol [48, 49]. Recombinant human MAO-A and MAO-B (Sigma-Aldrich) were used as enzyme sources, while kynuramine served as substrate for both enzyme isoforms. The enzyme reactions were carried out in potassium phosphate buffer (pH 7.4, 100 mM) and contained kynuramine (50 µM), the test inhibitors (0.003–100 µM) and MAO-A (0.0075 mg/mL) or MAO-B (0.015 mg/mL). After initiation with the addition of enzyme, the reactions were incubated for 20 min and at endpoint were treated with NaOH to terminate the enzyme reactions. The fluorescence intensity of 4-hydroxyquinoline, the product formed by MAO-catalyzed oxidation of kynuramine, was measured (λ_{ex} = 310 nm; λ_{em} = 400 nm). Sigmoidal plots of MAO catalytic rate versus logarithm of inhibitor concentration were constructed and the IC_{50} values were estimated and reported as the mean ± standard deviation (SD) of triplicate experiments.

4.5.1. Investigating reversibility of inhibition by dialysis

The reversibility of MAO-B inhibition by compound **19** was investigated by dialysis according to the literature protocol [48]. MAO-B (0.03 mg protein/mL) and the test compound at an

inhibitor concentration equal to 4 × IC_{50} were incubated for 15 min at 37 °C. The buffer was potassium phosphate buffer (100 mM, pH 7.4, 5% sucrose) and all incubations contained 4% DMSO as co-solvent. As negative control, MAO-B was incubated in the absence of inhibitor, while as positive control MAO-B was incubated with the irreversible inhibitor (*R*)-(-)-deprenyl [IC_{50}(MAO-B) = 0.019 μM], with the inhibitor concentration equal to 4 × IC_{50} [50]. The mixtures were subsequently dialyzed at 4 °C with the dialysis buffer being replaced with fresh buffer at 3 h and 7 h after the start of dialysis. After 24 h of dialysis, the mixtures were diluted twofold with the addition of the enzyme substrate, kynuramine, to yield an inhibitor concentration equal to 2 × IC_{50} and kynuramine concentration of 50 μM. These reactions were incubated for 20 min at 37 ºC, terminated with the addition of NaOH and the concentrations of 4-hydroxyquinoline were measured by fluorescence spectrophotometry as described above. For comparison, undialyzed mixtures of MAO-B and **19** were maintained at 4 °C for 24 h and the residual MAO-B activity was measured as for the dialyzed samples. All reactions were carried out in triplicate and the residual enzyme catalytic rates were expressed as mean ± SD.

4.5.2. Lineweaver-Burk plots

A set consisting of six Lineweaver-Burk plots was constructed for the inhibition of MAO-B by **19**. For this purpose, the following six inhibitor concentrations were used: 0 μM, ¼ × IC_{50}, ½ × IC_{50}, ¾ × IC_{50}, 1 × IC_{50} and 1¼ × IC_{50}. For each plot, kynuramine was used at 15–250 μM, and the concentration of MAO-B was 0.015 mg protein/mL. All enzyme reactions and activity measurements were carried out as described above for the dialysis experiments. The K_i value was estimated from a plot of the slopes of the Lineweaver-Burk plots versus inhibitor concentration (x-axis intercept equals $-K_i$).

4.6. Cholinesterases inhibition studies

To evaluate the capacity of the 4-(3-nitrophenyl)thiazol-2-ylhydrazones to inhibit ChE activity, the protocol of Ellman was used [51]. Electric eel AChE (EC 3.1.1.7), acetylthiocholine iodide (ASCh), 5,5'-dithio-bis-(2-nitrobenzoic acid) (DTNB) and the reference drug, galantamine, were purchased from Sigma-Aldrich (Milan, Italy). The assay was carried out with a double beam UV–Vis lambda 40 Perkin Elmer spectrophotometer using optical polystyrene cuvettes (10 x 10 x 45 mm, 340–800 nm optical transparency). The tested compounds were dissolved in DMSO and were added to the assay mixtures to yield a final DMSO content of <0.05%, a concentration that does not affect enzyme activity. This method is based on the cleavage of DTNB by

thiocholine (SCh), which is formed by the enzymatic hydrolysis of the ASCh. This cleavage yields 5-mercapto-2-nitrobenzoic with a strong yellow color and a maximum wavelength of absorbance at 412 nm. The changes in the absorbance at 25 °C were recorded between 0.5 and 1.5 min after substrate addition to the reaction mixture containing AChE, DTNB and the test compound in phosphate buffer (pH = 7.4). For the inhibition of BuChE, the sample solutions (50 µL) contained the test inhibitor, DTNB [5,5-dithio-bis(2-nitrobenzoic) acid] (125 µL) and the BuChE (horse serum butyrylcholinesterase, EC 3.1.1.8, Sigma) solution (25 µL) in Tris-HCl buffer (pH 8.0). The reactions were carried out in a 96-well microplate and incubated for 15 min at 25 °C. The reactions were initiated with the addition of butyrylthiocholine chloride (BTCl) (25 µL). The blank was prepared as above, but without enzyme (AChE or BuChE). The sample and blank absorbances were recorded at 405 nm after 10 min incubation at 25 °C. The absorbance of the blank was subtracted from that of the sample. The AChE/BuChE inhibition potency of each compound was expressed as percent inhibition obtained by the following equation:

$$inhibition(\%) = \frac{A_c - A_i}{A_c} \cdot 100$$

where A_i and A_c represent the change in the absorbance in the presence of inhibitor and absence of inhibitor, respectively.

4.7. Anti-oxidant activity evaluation

4.7.1. Phosphomolybdenum assay

The total anti-oxidant activity of the compounds was evaluated by phosphomolybdenum method according to Zengin *et al.* with slight modification [52]. The sample solution (0.3 mL) was combined with 3 mL of reagent solution (0.6 M sulphuric acid, 28 mM sodium phosphate and 4 mM ammonium molybdate) and the absorbance was recorded at 695 nm after 90 min incubation at 95 °C. The EC_{50}, which is the effective concentration at which the absorbance was 0.5, was calculated for each compound and trolox.

4.7.2. Radical scavenging activity

The radical scavenging effect of the compounds on the 1,1-diphenyl-2-picrylhydrazyl (DPPH) radical was estimated according to Zengin *et al.* [53]. The sample solution (1 mL) was added to 4 mL of a 0.004% solution of DPPH in methanol. The sample absorbance was recorded at 517 nm after 30 min incubation at room temperature in dark. The scavenging activity of the compounds on the ABTS radical cation [2,2'-azino-bis(3-ethylbenzothiazoline)-6-sulphonic acid] was

measured according to the method of Zengin *et al.* with slight modification [54]. Briefly, $ABTS^{\cdot+}$ was produced directly by reacting a 7 mM ABTS solution with 2.45 mM potassium persulphate and allowing the mixture to incubate for 12-16 h in the dark at room temperature. Prior to initiating the assay, the ABTS solution was diluted with methanol to an absorbance of 0.700 ± 0.02 at 734 nm. The sample solution (1 mL) was added to $ABTS^{\cdot+}$ solution (2 mL) and mixed, and the sample absorbance was recorded at 734 nm after 30 min incubation at room temperature. The corresponding IC_{50} value, which is the effective concentration at which 50% of DPPH/ABTS radicals are scavenged, was calculated for each compound and trolox.

4.7.3. Reducing power (CUPRAC and FRAP tests)

The cupric ion reducing activity (CUPRAC) was determined according to the method of Zengin *et al.* [55]. The sample solution (0.5 mL) was added to a premixed reaction mixture containing $CuCl_2$ (1 mL, 10 mM), neocuproine (1 mL, 7.5 mM) and NH_4Ac buffer (1 mL, 1 M, pH 7.0). Similarly, a blank was prepared by adding sample solution (0.5 mL) to a premixed reaction mixture (3 mL) without $CuCl_2$. The absorbances of the sample and blank were subsequently recorded at 450 nm after 30 min incubation at room temperature. The absorbance of the blank was subtracted from that of the sample.

The FRAP (ferric reducing antioxidant power) assay was carried out as described by Zengin *et al.* with slight modification [55]. The sample solution (0.1 mL) was added to the premixed FRAP reagent (2 mL) containing acetate buffer (0.3 M, pH 3.6), 2,4,6-tris(2-pyridyl)-*s*-triazine (TPTZ) (10 mM) in 40 mM HCl and ferric chloride (20 mM) in a ratio of 10:1:1 (*v*/*v*/*v*). The absorbance of the sample was subsequently recorded at 593 nm after 30 min incubation at room temperature. Both results were expressed as EC_{50} values.

Acknowledgments

This article is based upon work from COST Action CA15135, supported by COST.

Appendix A. Supplementary material

Top scored docking poses and elemental analysis results can be found at http://…….

References

[1] A. Wood-Kaczmar, S. Gandhi, N.W. Wood, Trends Mol. Med. 12 (2006) 521–528. doi: 10.1016/j.molmed.2006.09.007.

[2] A. Russell, A. Drozdova, W. Wang, M. Thomas, CNS Neurol. Disord. Drug Targets. 13 (2014) 1160-1168. doi: 10.2174/18715273136661409171227 39.

[3] A. Cavalli, M.L. Bolognesi, A. Minarini, M. Rosini, V. Tumiatti, M. Recanatini, C. Melchiorre, J. Med. Chem. 51 (2008) 347-372. doi: 10.1021/jm7009364.

[4] E. De Pablo-Fernández, D.P Breen., P.M. Bouloux, R.A. Barker, T. Foltynie, T.T. Warner, J. Neurol. Neurosurg. Psychiatry. 88 (2017) 176-185. doi: 10.1136/jnnp-2016-314601.

[5] L. Dezsi, L. Vecsei, CNS Neurol. Disord. Drug Targets. 16 (2017) 425-439. doi: 10.2174/1871527316666170124165222.

[6] M. Bortolato, K. Chen, J.C. Shih, Adv. Drug Deliver. Rev. 60 (2008) 1527-1533. doi: 10.1016/j.addr.2008.06.002.

[7] D. Robakis, S. Fahn, CNS Drugs 29 (2015) 433-441. doi: 10.1007/s40263-015-0249-8.

[8] M. Yamada, H. Yasuhara, Neurotoxicology 25 (2004) 215-221. doi: 10.1016/S0161-813X(03)00097-4.

[9] P. Hickey, M. Stacy, Front. Neurosci. 10 (2016) 173. doi: 10.3389/fnins.2016.00173.

[10] P. Calabresi, B. Picconi, L. Parnetti, M. Di Filippo, Lancet Neurol. 5 (2006) 974-983. doi: 10.1016/S1474-4422(06)70600-7.

[11] P.J. Reading, A.K. Luce, I.G. McKeith, Mov. Disord. 16 (2001) 1171-1174. doi: 10.1002/mds.1204.

[12] D. Aarsland, K. Laake, J.P. Larsen, C. Janvin, J. Neurol. Neurosurg. Psychiatry. 72 (2002) 708-712. doi: 10.1136/jnnp.72.6.708.

[13] A. Bolasco, R. Fioravanti, S. Carradori, Expert Opin. Ther. Pat. 15 (2005) 1763-1782.

[14] A. Bolasco, S. Carradori, R. Fioravanti, Expert Opin. Ther. Pat. 20 (2010) 909-939.

[15] S. Distinto, R. Meleddu, M. Yáñez, R. Cirilli, G. Bianco, M.L. Sanna, A. Arridu, P. Cossu, F. Cottiglia, C. Faggi, F. Ortuso, S. Alcaro, E. Maccioni, Eur. J. Med. Chem. 108 (2016) 545-552. doi: 10.1016/j.ejmech.2015.12.026.

[16] O.M. Bautista-Aguilera, A. Samadi, M. Chioua, K. Nikolic, S. Filipic, D. Agbaba, E. Soriano, L. de Andrés, M.I. Rodríguez-Franco, S. Alcaro, R.R. Ramsay, F. Ortuso, M. Yañez, J. Marco-Contelles, J. Med. Chem. 57 (2014) 10455-10463. doi: 10.1021/jm501501a.

[17] P. Chimenti, A. Petzer, S. Carradori, M. D'Ascenzio, R. Silvestri, S. Alcaro, F. Ortuso, J.P. Petzer, D. Secci, Eur. J. Med. Chem. 66 (2013) 221-227. doi: 10.1016/j.ejmech.2013.05.032.

[18] N. Desideri, R. Fioravanti, L. Proietti Monaco, M. Biava, M. Yáñez, F. Ortuso, S. Alcaro, Eur. J. Med. Chem. 59 (2013) 91-100. doi: 10.1016/j.ejmech.2012.11.006.

[19] S. Distinto, M. Yáñez, S. Alcaro, M.C. Cardia, M. Gaspari, M.L. Sanna, R. Meleddu, F. Ortuso, J. Kirchmair, P. Markt, A. Bolasco, G. Wolber, D. Secci, E. Maccioni, E. Eur. J. Med. Chem. 48 (2012) 284-295. doi: 10.1016/j.ejmech.2011.12.027.

[20] F. Chimenti, A. Bolasco, D. Secci, P. Chimenti, A. Granese, S. Carradori, M. Yáñez, F. Orallo, F. Ortuso, S. Alcaro, Bioorg. Med. Chem. 18 (2010) 5751-5723. doi: 10.1016/j.bmc.2010.06.007.

[21] F. Chimenti, E. Maccioni, D. Secci, A. Bolasco, P. Chimenti, A. Granese, O. Befani, P. Turini, S. Alcaro, F. Ortuso, M.C. Cardia, S. Distinto, J. Med. Chem. 50 (2007) 707-712. doi: 10.1021/jm060869d.

[22] S. Carradori, R. Silvestri, J. Med. Chem. 58 (2015) 6717-6732. doi: 10.1021/jm501690r.

[23] F. Chimenti, E. Maccioni, D. Secci, A. Bolasco, P. Chimenti, A. Granese, S. Carradori, S. Alcaro, F. Ortuso, M. Yáñez, F. Orallo, R. Cirilli, R. Ferretti, F. La Torre, J. Med. Chem. 51 (2008) 4874-4880. doi: 10.1021/jm800132g.

[24] F. Chimenti, D. Secci, A. Bolasco, P. Chimenti, A. Granese, S. Carradori, M. Yáñez, F. Orallo, M.L. Sanna, B. Gallinella, R. Cirilli, J. Med. Chem. 53 (2010) 6516-6520. doi: 10.1021/jm100120s.

[25] J. Cheung, M.J. Rudolph, F. Burshteyn, M.S. Cassidy, E.N. Gary, J. Love, M.C. Franklin, J.J. Height, J. Med. Chem. 55 (2012) 10282-10286. doi: 10.1021/jm300871x.

[26] J.M. Luco, J. Chem. Inf. Comput. Sci. 39 (1999) 396-404. doi: 10.1021/ci980411n.

[27] M. D'Ascenzio, S. Carradori, D. Secci, L. Mannina, A.P. Sobolev, C. De Monte, R. Cirilli, M. Yáñez, S. Alcaro, F. Ortuso, Bioorg. Med. Chem. 22 (2014) 2887-2895. doi: 10.1016/j.bmc.2014.03.042.

[28] M. D'Ascenzio, P. Chimenti, M.C. Gidaro, C. De Monte, D. De Vita, A. Granese, L. Scipione, R. Di Santo, G. Costa, S. Alcaro, M. Yáñez, S. Carradori, J. Enzyme Inhib. Med. Chem. 30 (2015) 908-919. doi: 10.3109/14756366.2014.987138.

[29] C. Aldrich, C. Bertozzi, G.I. Georg, L. Kiessling, C. Lindsley, D. Liotta, K.M. Jr Merz, A. Schepartz, S. Wang, J. Med. Chem. 60 (2017) 2165-2168. doi: 10.1021/acs.jmedchem.7b00229.

[30] http://zinc15.docking.org/patterns/home.

[31] J.B. Baell, G.A. Holloway, J. Med. Chem. 53 (2010) 2719–2740. doi: 10.1021/jm901137j; http://www.cbligand.org/PAINS.

[32] D. Lagorce, O. Sperandio, H. Galons, M.A. Miteva, B.O. Villoutreix, BMC Bioinformatics 9 (2008) 396-405. doi: 10.1186/1471-2105-9-396; http://fafdrugs3.mti.univ-paris-diderot.fr.

[33] Schrödinger, LLC, New York, NY, 2015.

[34] Maestro, version 10.4, Schrödinger, LLC, New York, NY, 2015.

[35] G.A. Kaminski, R.A. Friesner, J. Tirado-Rives, W.J. Jorgensen, J. Phys. Chem. B. 105 (2001) 6474-6487. doi: 10.1021/jp003919d.

[36] W. Hasel, T.F. Hendrickson, W.C. Still, Tetrahedron Comput. Methodol. 1 (1988) 103-116. doi: 10.1016/0898-5529(88)90015-2.

[37] H.B. Berman, J. Westbrook, Z. Feng, G. Gilliland, T.N. Bhat, H. Weissig, I.N. Shindyalov, P.E. Bourne, Nucleic Acids Res. 28 (2000) 235-242. doi: 10.1093/nar/28.1.235.

[38] S.Y. Son, J. Ma, Y. Kondou, M. Yoshimura, E. Yamashita, T. Tsukihara, Proc. Natl. Acad. Sci. USA 105 (2008) 5739-5744. doi: 10.1073/pnas.0710626105.

[39] C. Binda, J. Wang, L. Pisani, C. Caccia, A. Carotti, P. Salvati, D.E. Edmondson, A. Mattevi, J. Med. Chem. 50 (2007) 5848-5852. doi: 10.1021/jm070677y.

[40] J. Cheung, E.N. Gary, K. Shiomi, T.L. Rosenberry, ACS Med. Chem. Lett. 4 (2013) 1091-1096. doi: 10.1021/ml400304w.

[41] Y. Nicolet, O. Lockridge, P. Masson, J.C. Fontecilla-Camps, F. Nachon, J. Biol. Chem. 278 (2003) 41141-41147. doi: 10.1074/jbc.M210241200.

[42] Jaguar, version 9.0, Schrödinger, LLC, New York, NY, 2015.

[43] GRID, version 22a. Molecular Discovery L.T.D. (www.moldiscovery.com).

[44] P.J. Goodford, J. Med. Chem. 28 (1985) 849-857. doi: 10.1021/jm00145a002.

[45] QikPop, version 4.6, Schrödinger, LLC, New York, NY, 2015.

[46] Glide, version 6.9, Schrödinger, LLC, New York, NY, 2015.

[47] S. Carradori, D. Rotili, C. De Monte, A. Lenoci, M. D'Ascenzio, V. Rodriguez, P. Filetici, M. Miceli, A. Nebbioso, L. Altucci, D. Secci, A. Mai, Eur. J. Med. Chem. 80 (2014) 569-578. doi: 10.1016/j.ejmech.2014.04.042.

[48] S. Mostert, A. Petzer, J.P. Petzer, ChemMedChem. 10 (2015) 862-873. doi: 10.1002/cmdc.201500059.

[49] S. Mostert, A. Petzer, J.P. Petzer, Bioorg. Med. Chem. Lett. 26 (2016) 1200-1204. doi: 10.1016/j.bmcl.2016.01.034.

[50] A. Petzer, B.H. Harvey, G. Wegener, J.P. Petzer, Toxicol. Appl. Pharmacol. 258 (2012) 403-409. doi: 10.1016/j.taap.2011.12.005.

[51] G.L. Ellman, K.D. Courtney, V. Jr Andres, R.M. Featherstone, Biochem. Pharmacol. 7 (1961) 88-95. doi: 10.1016/0006-2952(61)90145-9.

[52] G. Zengin, C. Sarikurkcu, A. Aktumsek, R. Ceylan, O. Ceylan, Ind. Crop. Prod. 53 (2014) 244-251. doi: 10.1016/j.indcrop.2013.12.043.

[53] G. Zengin, C. Sarikurkcu, E. Gunes, A. Uysal, R. Ceylan, S. Uysal, H. Gungor, A. Aktumsek, Food Funct. 6 (2015) 2794-2802. doi: 10.1039/c5fo00665a.

[54] A. Aktumsek, G. Zengin, G.O. Guler, Y.S. Cakmak, A. Duran, Food Chem. Toxicol. 55 (2013) 290-296. doi:10.1016/j.fct.2013.01.018.

[55] G. Zengin, R. Ceylan, G.O. Guler, S. Carradori, S. Uysal, A. Aktumsek, Curr. Enzyme Inhib. 12 (2016) 177-182. doi: 10.2174/1573408012666160127231058.

ACCEPTED MANUSCRIPT

Highlights

- A rational drug design approach suggested the synthesis of new MAO-B inhibitors
- The compounds displayed dual MAO-B and AChE inhibitory activity
- Their anti-oxidant activity could enhance the pharmacological application in neurodegenerative disorders
- Pharmacokinetic properties of each compound were theoretically predicted
- Compound **19** acted as a competitive and reversible MAO-B inhibitor

ACCEPTED MANUSCRIPT